JOURNAL OF APPLIED ELECTROCHEMISTRY 23 (1993) 500–507

Galvanic black anodizing on Mg–Li alloys

A. K. SHARMA, R. UMA RANI, H. BHOJARAJ, H. NARAYANAMURTHY

Thermal Systems Group, ISRO Satellite Centre, Vimanapura P.O., Bangalore 560 017, India

Received 4 December 1991; revised 14 July 1992; accepted 17 July 1992

A process of galvanic black anodizing on Mg–Li alloys was studied. The influence of various operating parameters, namely galvanic current density, voltage, pH, electrolyte concentration, operating temperature, anodizing time and heat treatment on the anodic film formation have been investigated to optimize the process. The deposits were characterized by optical and scanning electron microscopy, adhesion tests, corrosion studies, thickness measurement and microhardness evaluation. The space worthiness of the coatings has been evaluated by humidity, thermal cycling and thermo-vacuum tests and measurement of optical properties. The results of all these studies are clearly indicative that the black anodizing process described herein is extremely suitable for ground, as well as space, applications.

Nomenclature

α_s	Solar absorbance
ε_{ir}	Infrared emittance
VHN	Vickers hardness number

1. Introduction

Magnesium–lithium alloys are the lightest structural metallic alloys known today. The addition of 10–15% by weight of lithium (density 0.5 g cm^{-3}) to magnesium results in an alloy with a density of 1.3 to 1.4 g cm^{-3} leading to a considerable weight saving. These alloys are 25% lighter than conventional magnesium alloys.

The binary magnesium–lithium alloys, although light and ductile, are not strong. Addition of aluminum results in considerable improvement in strength, primarily due to the formation of the $MgLi_2Al$ metastable phase [1]. McDonald [1–3] has reported that the best combination of mechanical strength and ductility can be obtained with addition of aluminium in an atomic percentage greater than 0.05. Development and production of a Mg–Li alloy, designated as MLA with 10–13% Li, 1.25–1.75% Al, and balanced Mg % by weight is presently being carried out at DMRL, Hyderabad. The combination of light weight and outstanding stiffness has prompted the use of Mg–Li alloys in the aerospace field primarily for housing electronic packages [4].

Although Mg–Li alloys were first reported in the sixties, no evidence for their successful application is available, in spite of their outstanding properties. This is because the alloys are highly sensitive to atmospheric corrosion due to the inclusion of lithium. The Mg–Li alloys react severely, even at room temperature, when exposed to the atmosphere or aqueous solutions. Further, no literature on successful surface treatment of these alloys is available. We have undertaken the development of protective coatings on Mg–Li alloys and have reported previously the successful development of a chromate conversion coating [5] and gold plating procedures [4, 6].

The present paper describes the process of galvanic black anodizing of Mg–Li alloys.

2. Experimental Details

2.1. *Anodizing process*

Galvanic black anodizing on Mg–Li alloy MLA was investigated on samples sized 70 mm × 40 mm × 8 mm using the following sequence of operations:

(i) Ultrasonic solvent degreasing in isopropanol for 5–10 min.

(ii) Alkaline cleaning
Sodium hydroxide, NaOH: 50 g dm^{-3}
Trisodium orthophosphate, $Na_3PO_4 . 12H_2O$: 10 g dm^{-3}
Temperature: 60 ± 5° C
Time: 5–10 min
Post treatment: Water rinse

(iii) Acid pickling
Chromic acid, CrO_3: 500 g dm^{-3}
Ferric nitrate, $Fe(NO_3)_3 . 9H_2O$: 1 g dm^{-3}
Potassium fluoride, KF: 0.5–1.0 g dm^{-3}
Time: 3–5 min
Post treatment: Water rinse

(iv) Fluoride activation
Dipping the specimen in hydrofluoric acid (40%) 50 ml dm^{-3} for 10 min, followed by water rinsing.

(v) Black anodizing
Potassium dichromate, $K_2Cr_2O_7$: 25 g dm^{-3}
Ammonium sulphate, $(NH_4)_2 SO_4$: 25 g dm^{-3}
pH: 5.5
Temperature: 24 ± 1° C
Cathode: anodizing tank (stainless steel)
Anode to cathode area ratio: 1/10
Galvanic current/voltage: 0.8–2.4 mA cm^{-2}
1.2–3.6 mV cm^{-2}
Time: 60 min

0021-891X

The pH was adjusted upward with dilute ammonium hydroxide and downward with dilute sulphuric acid.

(vi) Heat treatment at 70° C for 2 h in an electric oven with facility for clean hot air circulation.

Distilled or deionized water was used for solution preparation. All the chemicals used were laboratory reagent grade. The test specimens were mechanically agitated during the process.

2.2. *Instrumentation and measurement techniques*

The morphological studies of the anodic coating were carried out with a Reichert Jung MeFz microscope (Austria), and a JEOL JSM-840-A scanning electron microscope (Japan).

The humidity tests were conducted in a thermostatically controlled Heraeus Votsch type 08, 500 (Germany), humidity chamber. The relative humidity in the chamber was maintained within 95 ± 0.5% at 50° C.

The corrosion resistance studies were carried out by immersion of test specimens in 5% sodium chloride solution at pH 7.0. After 8 h of immersion, the coating was carefully examined for discolouration or formation of any corrosion spots on the surface.

Thermal cycling tests, designed to evaluate the effect of cycling temperature likely to be encountered throughout the life span of a spacecraft, was carried out in a thermostatically controlled Brabender Real Test Umweltsimulatoren Hot and Cold Chamber (Germany). A total of 1000 cycles was applied. A cycle consisted of lowering the temperature to −45° C, a dwell of 5 min, raising the temperature to 80° C and a dwell of 5 min.

To examine the effect of cycling temperature on the coating in vacuum (space environment) a thermovacuum test was performed in a thermostatically controlled Hind high vacuum chamber, model-VS-4 (India). The test consisted of lowering the temperature to −45° C, a dwell of 2 h and raising the temperature to 80° C and a dwell of 2 h. A total of 10 cycles of hot and cold soak was applied. A vacuum level of better than 10^{-5} torr was maintained inside the test chamber throughout the test period.

After humidity, corrosion resistance, thermal cycling and thermovacuum tests, the coatings were examined visually and under magnification (4×) for any degradation in physical appearance and their optical properties were measured.

Adhesion of the anodic coating was evaluated by a Scotch tape peel off test. The test consisted of scribing through the deposit to the base metal 11 parallel lines with a sharp blade approximately 2 mm apart. Another 11 lines were scribed perpendicular to and across the first 11 lines. The resulting pattern was 100 squares of 4 mm^2 each. Masking tape of ~25 mm width type 3M-500 (pressure 200 $g\,cm^{-1}$ width) was then applied over the anodic film by passing a 2 kg rubber covered roller over the tape twice. The tape was then removed quickly in a direction normal to the surface and the test specimens were examined visually for any coating removal. This test was also conducted after humidity, corrosion resistance, thermal cycling and thermovacuum tests.

The thickness of the anodic coating was measured using an Isoscope MP 2B-T3 3B, Helmut Fischer (Germany), coating thickness tester. This instrument works on the eddy current principle and is used to measure the thickness of non conductive coatings on conductive substrates. The thickness of the film on a few randomly selected samples was also examined under a graduated scale microscope after microsectioning and metallographically polishing the cross section of the test coupons.

The microhardness of the coatings was measured with a Shimadzu microhardness Tester Type M, (Kyoto, Japan), using a diamond indentor. Vickers hardness numbers were obtained by averaging seven measurements on each specimen with a load of 15 g.

The optical properties, namely solar reflectance and infrared emittance of the coatings were measured using a solar reflectometer version 50, model SSR-ER and an emissometer model RD1, respectively, from Devices and Services Co. (USA). Both these instruments provide an average value of solar absorptance and infrared emittance digitally over the entire solar or infrared region. The solar spectrum of the anodic coating was recorded on a Varian spectrophotometer (Australia), in the 0.2 to 2.3 μm region while infrared spectra was obtained in the 2.5 to 50 μm region with a Perkin Elmer 580-B infrared spectrophotomer, (USA).

3. Mechanism of film depostion

The coating is formed by a chemical reaction between the magnesium–lithium alloy surface and hexavalent chromium. The alloy metals are oxidized by the hexavalent chromium, which is reduced to the trivalent state. Essentially this is a controlled reduction–oxidation reaction. When the alloy specimen is immersed in the anodizing solution and is connected to the stainless steel anodizing tank, the alloy surface dissolves to a small extent in the solution, a flow of current starts from alloy specimen (anode) to stainless steel tank (cathode). The chemistry of film deposition can be represented by the following equations:

Electrolytic reactions (ionization)

$$K_2Cr_2O_7 \longrightarrow 2K^+ + Cr_2O_7^{2-}$$

$$(NH_4)_2SO_4 \longrightarrow 2NH_4^+ + SO_4^{2-}$$

$$H_2O \longrightarrow H^+ + OH^-$$

Anodic reactions

$$Mg^0 \longrightarrow Mg^{2+} + 2e^-$$

$$2Mg^{2+} + 2Cr_2O_7^{2-} + 6OH^-/3SO_4^{2-} \longrightarrow 2MgCrO_4 + 2Cr(OH)_3/Cr_2(SO_4)_3 + 3O_2 + 6e^-$$

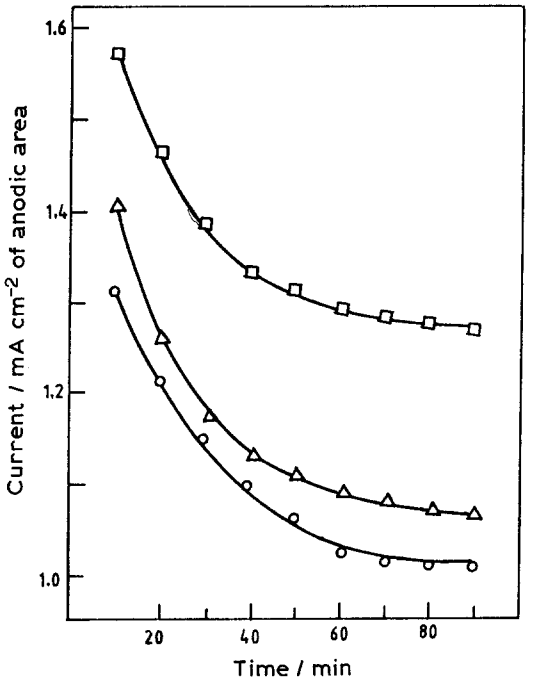

Fig. 1. Variation in galvanic current with time at various operating temperatures: (○) 24° C, (△) 40° C, (□) 60° C.

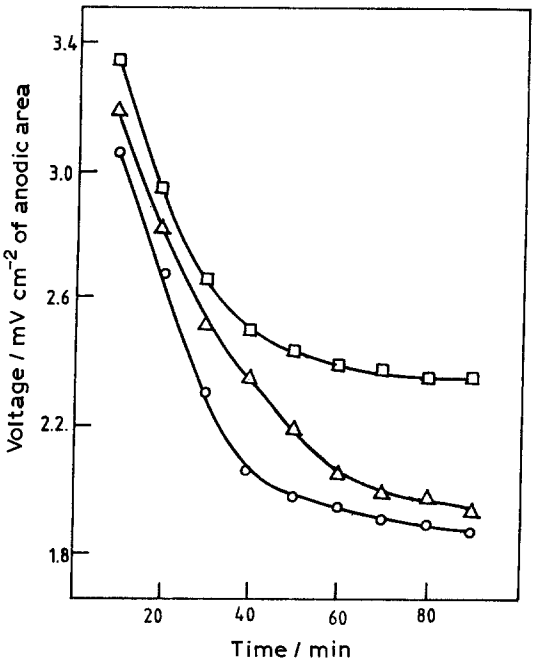

Fig. 2. Variation in galvanic voltage with time at various operating temperatures: (○) 24° C, (△) 40° C, (□) 60° C.

Cathodic reactions

$$K^+ + OH^- \longrightarrow KOH$$

$$NH_4^+ + OH^- \longrightarrow NH_4OH$$

$$2H^+ + 2e^- \longrightarrow H_2\uparrow$$

The dissolution of the alloy surface in the solution causes a pH rise at the solid–liquid interface [7, 8]. This results in the precipitation of a thin complex chromium metal gel on the surface composed of hexavalent and trivalent chromium and the substrate metal. This gel is very soft when formed and therefore the coated work must be carefully handled. After drying, the coating becomes harder.

4. Results and discussion

4.1. *Process optimization*

4.1.1. Variation in galvanic current density and voltage. The behaviour of galvanic anodic current and voltage with time at electrolyte temperatures of 24, 40 and 60° C is shown in Figs. 1 and 2, respectively. As expected, owing to the formation of the anodic coating, both the current density and voltage fell with time and reached more or less steady state after 2 h of electrolysis. Further, due to the higher conductivity and increase in rate of dissolution of the alloy in the electrolyte at higher temperatures both the current density and voltage tended to be higher with higher operating temperatures.

4.1.2. Effect of electrolyte pH. The influence of electrolyte pH on the nature and growth of the deposits was investigated. The effect of electrolyte pH on the thickness of anodic coating is shown in Fig. 3. As the electrolyte pH increased, the thickness of the anodic coating decreased. This is attributed to the fact that at lower pH the alloy dissolves in the electrolyte at a faster rate, producing higher galvanic current which results in a rapid film growth. At pH 7.0, the test coupons were only partially covered by the anodic coating and no coating was obtained at pH 9.0 or above. At pH down to 4.0 due to the rapid rate of

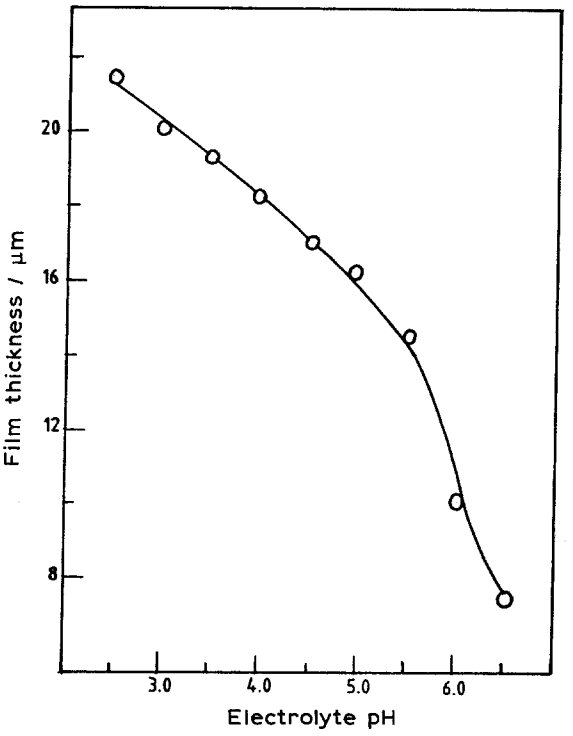

Fig. 3. Effect of electrolyte pH on the thickness of anodic coating.

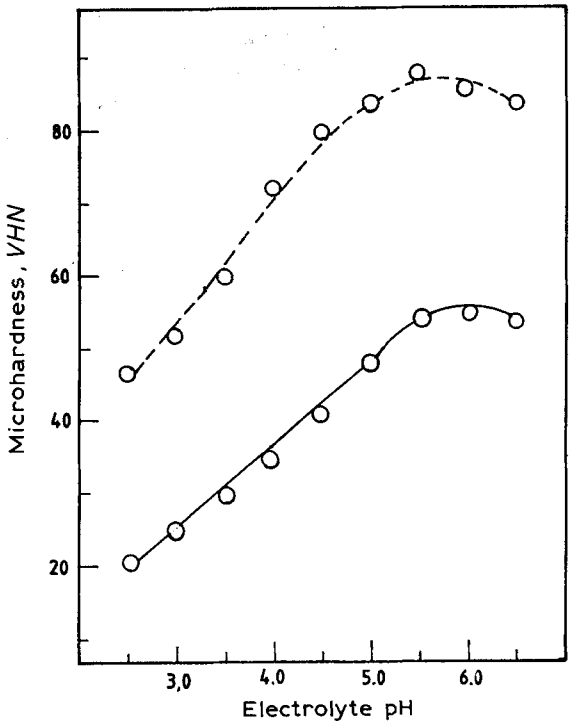

Fig. 4. Effect of electrolyte pH on the microhardness of anodic coating: (——) without heat treatment; (– – –) after heat treatment.

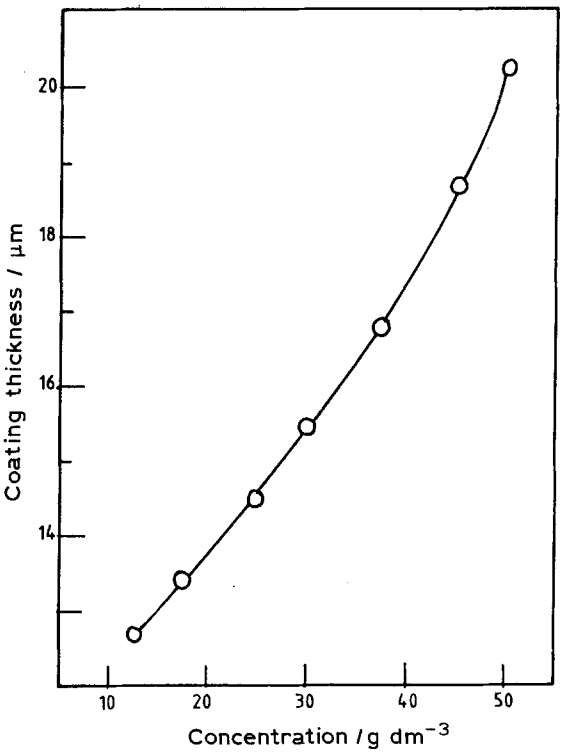

Fig. 5. Effect of electrolyte concentration on the thickness of anodic coating.

deposition the coatings obtained were very rough and powdery.

Figure 4 depicts the effect of electrolyte pH on the microhardness of the anodic coating. From pH 2.5 to 5.5, the microhardness of the coating increased almost linearly with increase in pH. This trend changed at pH value above 5.5 where a slight drop in microhardness was observed.

It is apparent from the above discussion that the optimum pH for galvanic black anodizing on Mg–Li alloy is 5.5. The experiment results however, showed that satisfactory coating can be obtained at pH above 4.5 and below 6.5. The effect of pH on the optical properties of the coating was almost insignificant in the pH range 2.5 to 6.0. However, a sharp drop (> 0.10) in infrared emittance of the coatings obtained at pH 6.5 and above was observed.

4.1.3. Effect of electrolyte concentration. The rate of film deposition is generally higher for higher concentration electrolytes. This is primarily attributed to the presence of higher contents of reactants and partly because of higher conductivity of concentrated electrolyte. The flow of the galvanic current is faster in the higher concentration electrolytes. The effect of electrolyte concentration at a constant pH 5.5 on the thickness of the anodic coating is presented in Fig. 5. It is evident from the figure that the coating thickness increased almost linearly with the increase in electrolyte concentration.

Figure 6 depicts the effect of electrolyte concentration on the microhardness of the coatings. The microhardness of the anodic coating increased initially and subsequently dropped with the increase in electrolyte concentration. The maximum hardness value was obtained for the concentration of $25\,g\,dm^{-3}$.

The optical microscope studies revealed that the throwing power of dilute electrolytes with concentration $< 15\,g\,dm^{-3}$ were not satisfactory and the coatings formed were often non uniform and patchy. Further the pitting spots were observed in the coatings obtained with electrolytes of concentration higher than $35\,g\,dm^{-3}$. These results clearly indicate that the

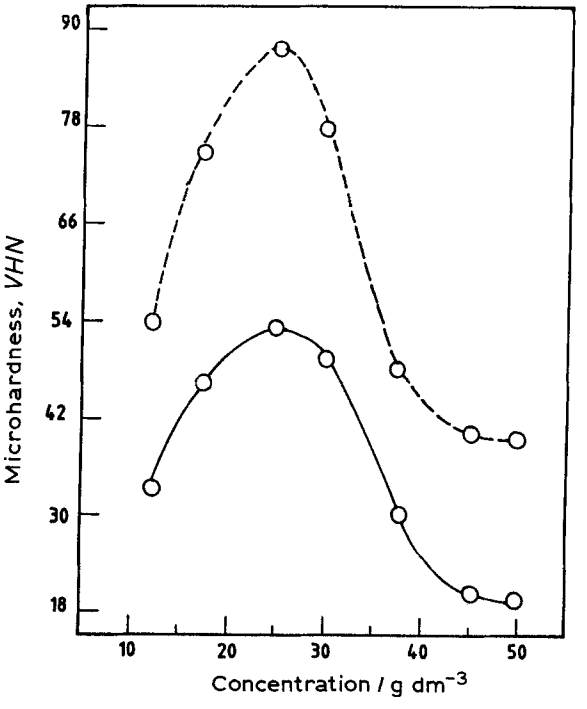

Fig. 6. Effect of electrolyte concentration on the microhardness of anodic coating: (——) without heat treatment; (– – –) after heat treatment.

Table 1. Effect of process conditions on physico-optical properties of anodic coatings (Anodizing time 60 min)

Process conditions	*Thickness* μm/AHT	*Microhardness (VHN)* BHT	AHT	α_s	$\varepsilon_{i.r.}$
1. *Effect of electrolyte temperature (°C)* Electrolyte: $K_2Cr_2O_7$ 25 g dm^{-3}, $(NH_4)_2SO_4$ 25 g dm^{-3}, pH 5.5]					
24	14.5	53	88	0.953	0.93
40	21.3	37	45	0.954	0.93
60	25.3	28	34	0.954	0.93
2. *Effect of electrolyte pH* [Electrolyte: $K_2Cr_2O_7$ 25 g dm^{-3}, $(NH_4)_2SO_4$ 25 g dm^{-3}, temp. 24° C]					
2.5	21.5	22	47	0.957	0.93
3.0	20.2	25	52	0.951	0.93
3.5	19.4	29	60	0.952	0.93
4.0	18.4	36	72	0.953	0.93
4.5	17.1	41	80	0.950	0.93
5.0	16.4	48	84	0.948	0.93
5.5	14.5	53	88	0.953	0.93
6.0	10.0	53	86	0.955	0.86
6.5	7.3	52	84	0.957	0.80
3. *Effect of electrolyte concentration (g dm^{-3} of $K_2Cr_2O_7$ and $(NH_2)_2$ SO_4)* [Temp. 24° C, pH 5.5]					
12.5	12.7	33	54	0.959	0.91
17.5	13.4	46	75	0.957	0.92
25.0	14.5	53	88	0.953	0.93
30.0	15.5	50	78	0.956	0.93
37.5	16.8	30	48	0.957	0.93
45.0	18.7	22	46	0.958	0.93
50.0	20.3	20	45	0.959	0.93
4. *Effect of Electrolyte constituent* [Each constituent 25 g dm^{-3}, Temp. 24° C, pH 5.5]					
$Na_2Cr_2O_7$ + $(NH_4)_2SO_4$	15.0	32	71	0.956	0.89
$Na_2Cr_2O_7$ + Na_2SO_4	14.0	35	82	0.954	0.87
$K_2Cr_2O_7$ + Na_2SO_4	14.3	40	86	0.958	0.88
5. *Effect of addition agents* [Electrolyte $K_2Cr_2O_7$ 25 g dm^{-3}, $(NH_4)_2SO_4$ 25 g dm^{-3}; pH 5.5, temp. 24° C]					
KF 1 g dm^{-3}	13.8	56	96	0.951	0.80
6. *Effect of sealing*					
Boiling water	14.5	46	68	0.952	0.88
$K_2Cr_2O_7$(1%)–NH_4HF_2(5%)	14.5	58	92	0.954	0.86
Na_2SiO_3 200 g dm^{-3}	14.5	64	103	0.954	0.83

BHT Before heat treatment; AHT After heat treatment at 70° C for 2 h

optimum electrolyte concentration is: potassium dichromate 20–30 g dm^{-3} and ammonium sulphate 20–30 g dm^{-3}. No effect of electrolyte concentration in the range of investigation (12.5–50.0- g dm^{-3}) was noticed on the optical behaviour of the anodic coating.

4.1.4. Effect of electrolyte constituents and sealing. Experiments were conducted by replacing potassium dichromate with sodium dichromate and ammonium sulphate with sodium or potassium sulphate, (each constituent 25 g dm^{-3}) at a constant pH of 5.5 and temperature 24 ± 1° c. The results of these experiments are presented in Table 1. The comparison of these results indicates that there was no appreciable change in the growth and properties of the anodic coating obtained with different electrolyte combinations. It was evident however, from the appearance and uniformity of the coatings that the potassium dichromate–amonium sulphate electrolyte provided better throwing power. This electrolyte system was also found to yield the coatings with highest infrared emittance. No change in solar absorptance of the anodic coating obtained with different electrolytes was however, observed.

The influence of post deposition sealing and addition agents on the physico-optical properties of the anodic coating has also been investigated. The microhardness of the anodic coating was found to improve by some of these treatments but a drop in infrared emittance by 5 to 10% was observed. These results are presented in Table 1.

4.1.5. Effect of electrolyte temperature. In most of the chemical reactions the rate of reaction is dependent on the bath temperature. At higher temperatures the deposition rate is generally higher primarily due to the

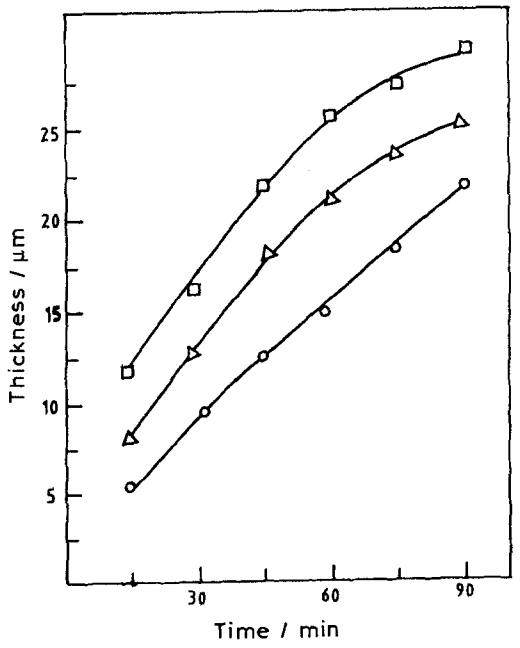

Fig. 7. Variation in anodic coating thickness with time at various operating temperatures: (○) 24° C, (△) 40° C, (□) 60° C.

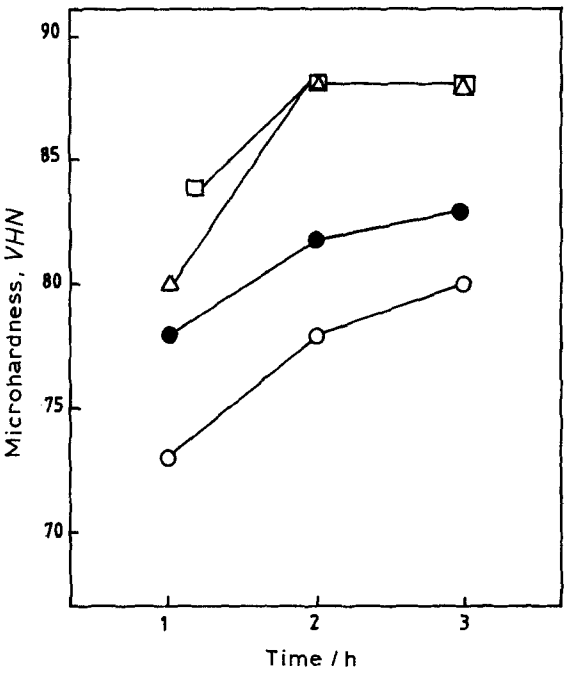

Fig. 9. Effect of heat treatment on the microhardness of anodic coating: (○) 50° C, (●) 60° C, (△) 70° C, and (□) 80° C.

increase in activation energy and conductivity of solutions. Figure 7 shows the variation in the anodic coating thickness with time at various operating temperatures 24° C, 40° C and 60° C. It is apparent from this figure that the rate of deposition increased with increase in electrolyte temperatures.

Figure 8 depicts the variation in microhardness of the anodic coating with thickness at various operating temperatures with and without heat treatment. It clearly indicates that the microhardness of the anodic coating decreased as the bath temeprature increased for the same film thickness. However, no effect of electrolyte temperature (24–60° C) was observed on the optical properties of the coatings.

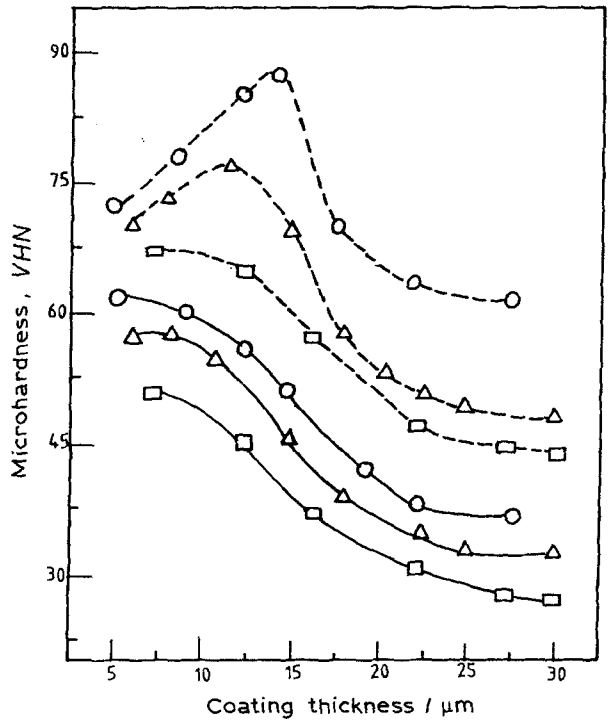

Fig. 8. Variation in microhardness of anodic coating with thickness at various operating temperatures: (○) 24° C, (△) 40° C, (□) 60° C, (——) without heat treatment; (- - -) after heat treatment.

4.1.6. Effect of heat treatment.. The hardness of the anodic coating was found to increase by post deposition heat treatment. The effect of heat treatment on the microhardness of the coatings is shown in Fig. 9.. It is clear from this graph that the optimum microhardness of the coatings can be achieved by heat treatment at 70° C for 2 h. The heat treatment of the coatings above 70° C does not result in any significant improvement in microhardness.

The optical properties of the coatings remain unchanged after heat treatment at 50–80° C. A slight degradation in infrared emittance of coatings was observed after heat treatment at 90° C for 2 h. When examined under 500×, a macrocrack formation was noticed, thus the film lost its protective values.

The effect of process conditions on physico-optical properties of the anodic coating is presented in Table 1.

4.2. *Adhesion and environmental stability*

Black anodic coatings were found to have excellent adhesion in the Scotch tape peel test. No detachment of film was observed from any point as per MIL-C-81706 specifications. To evaluate the performance of the anodic coating during pre and post launch environments the test coupons were subjected to humidity, corrosion resistance, thermal cycling and thermovacuum performance tests. The humidity and corrosion resistance tests were carried out to examine the resistance of the anodic coating to corrosive pre launch atmosphere while the thermal cycling and thermovacuum tests were designed to evaluate the effect of on-orbit cycling temperature of spacecraft on

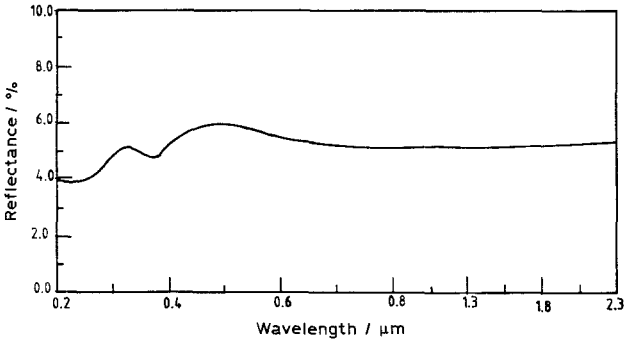

Fig. 10. Solar reflectance spectra of anodic coating.

the physio-optical properties of the anodic film [9].

The black anodic coating withstood all these severe environmental tests without any degradation in physical appearance and optical properties. These results are indicative of excellent environmental stability of the coating for ground as well as space applications.

4.3. *Optical properties*

In the absence of an atmosphere, heat exchange in space is limited to radiation. The black anodic coating with high absorptance and emittance values helps in minimizing temperature gradients across all the internal components of the spacecraft. The influence of various operating parameters on the optical properties of the coating has been discussed in Section 4.1. The solar and infrared spectra of the coatings are presented in Figs. 10 and 11, respectively.

4.4. *Morphological studies*

The microstructure of the anodic coating was examined using optical and scanning electron microscopy. Coatings of this type are usually considered to have a gel-like structure as formed, but, after drying, they harden and crack to give a microcracked pattern. Figure 12 shows the scanning electron micrographs of the anodic coating. The film had a 'mud-crack' pattern. After heat treatment these microcracks became wider and edge curling of the blocks of the coating occurred. This probably resulted due to the dehydration and shrinkage of the film [10]. The term microcrack refers to a crack that does not extend from the base metal to the surface of the deposit.

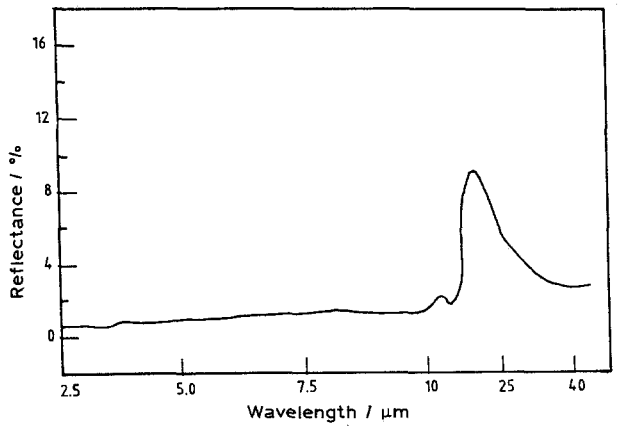

Fig. 11. Infrared reflectance spectra of anodic coating.

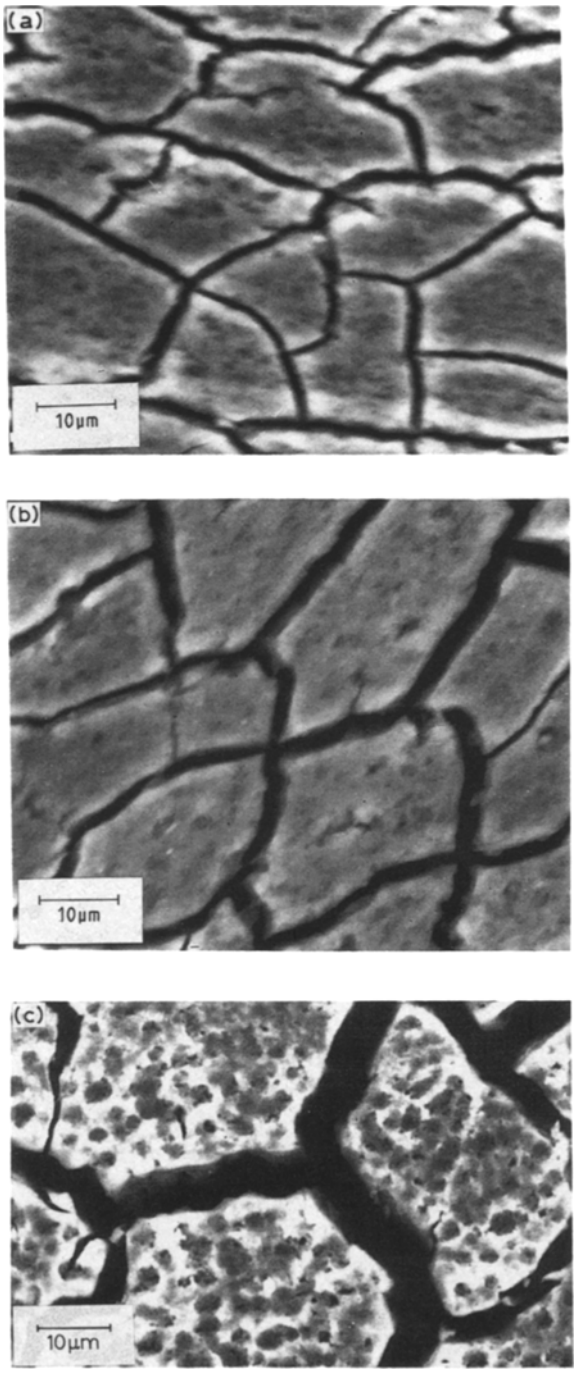

Fig. 12. Scanning electron micrographs of black anodic coating (a) without heat treatment (b) after heat treatment at 70° C (c) at higher thickness: coating thickness, 14 μm for (a) and (b), 25 μm for (c).

The cross section of anodized specimen was metallographically polished and examined by optical microscopy in the unetched condition. It is apparent from the photomicrograph of a cross section shown in Fig. 13 that the anodic coating had a good adhesion to the substrate. The good uniformity of the black anodic coating showed that the electrolyte used for anodizing had excellent throwing power.

5. Conclusions

(i) The black anodic coating on Mg–Li alloys was obtained under the following electrolyte composition

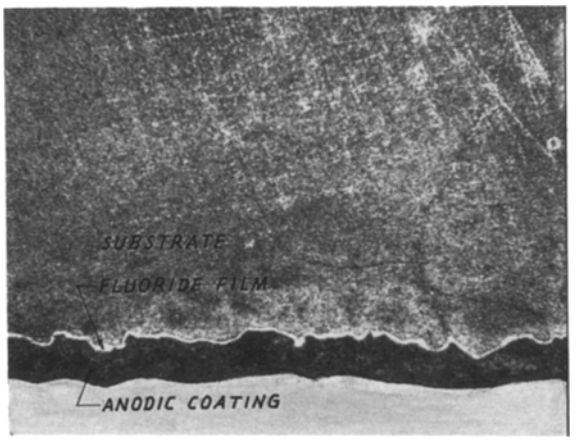

Fig. 13. Photomicrograph of the cross section of anodized specimen (480 ×).

and operating conditions

Potassium dichromate, $K_2Cr_2O_7$: 25 g dm^{-3}
Ammonium sulphate, $(NH_4)_2SO_4$: 25 g dm^{-3}
pH: 5.5
Cathode: Anodizing tank (stainless steel)
Temperature: 24 ± 1° C
Galvanic current/voltage: 0.8–2.4 mA cm^{-2}; 1.2–3.6 mV cm^{-2}
Time: 60 min

(ii) The process yielded satisfactory coatings in a wide range of electrolyte pH (4.5–6.5) and concentration (20–30 g dm^{-3} of each constituent). Further, as these coatings provided high solar absorptance and thermal emittance (> 0.90) values these are extremely suitable for thermal control application.

Acknowledgements

The authors are grateful to A.V. Patki (Deputy Director, Mechanical Systems), V.K. Kaila (Deputy Project Director INSAT-2), and K. Kasthurirangan (Director, ISRO Satelllite Centre) for their constant encouragement during the study. Thanks are also due to R.P. Sahu, M.R. Suresh and B.V. Bhoopalakrishna for their cooperation.

References

[1] J. McDonald, *Trans, ASM* **61** (1968) 505.
[2] *Idem, J. Inst. Metals* **97** (1969) 353.
[3] *Idem, ibid.* **99** (1971) 24.
[4] A. K. Sharma, *Met. Finish.* **89** (July 1991) 16.
[5] *Idem, ibid.* **87** (Feb 1989) 73.
[6] *Idem, ibid.* **86** (Dec 1988) 83.
[7] Jack Kindler, 'Chromate Conversion coatings', American Electroplaters' Soc. Inc., FL (1986) p. 6.
[8] L. J. Durney (Ed.) 'Electroplating Engineering Handbook' Van Nostrand Reinhold, New York (1984) p. 390.
[9] A. K. Sharma, *Thin Solid Films* **208** (1992) 48.
[10] N. R. Short, J. K. Dennis and S. O. Agbonlahor, *Trans. Inst. Met. Finish.* **66** (Aug. 1988) 107.